# High-Performance RF Devices and Components on Flexible Cellulose Substrate by Vertically Integrated Additive Manufacturing Technologies

Chiara Mariotti, *Member, IEEE*, Federico Alimenti, *Senior Member, IEEE*, Luca Roselli, *Senior Member, IEEE*, and Manos M. Tentzeris, *Fellow, IEEE*

*Abstract*—This paper aims to demonstrate that novel additive manufacturing (AM) technologies like metal adhesive laminate and multilayer inkjet printing can be effectively exploited to fabricate high-performing radio-frequency passive components on flexible substrates. Both processes are substrate independent and therefore suitable for manufacturing circuits on several unconventional materials, such as photo-paper. In addition, their complementary features can be combined to develop a novel hybrid process. Proof-of-concept AM prototypes of passive components, such as capacitors and inductors, exhibiting quality factors over 70, never achieved before on paper, and self-resonant frequencies beyond 4 GHz are described. The maximum inductance and capacitance per unit area are 1.4 nH/mm$^2$ and 6.5 pF/mm$^2$, respectively. Moreover, an AM RF mixer with a conversion loss below 10 dB is demonstrated still on paper substrate. The mixer, fabricated with the copper adhesive laminate method, operates at 1 GHz and exploits a lumped balun transformer connected to two packaged diodes in series.

*Index Terms*—Additive manufacturing (AM), copper adhesive laminate, flexible electronics, green electronics, inkjet printing, Internet of Everything (IoE), Internet of Things (IoT), passive components.

## I. Introduction

CISCO reported about the market forecast for Internet of Things (IoT) in 2011 as "IoT will change everything, including ourselves (...) there will be 50 billion devices connected to the Internet by 2020" [1]. Another report from Verizon [2] states that the IoT "is founded on familiar technologies—like sensors, networking, and cloud computing—but its potential for transformation is incredible" and it has already increased the connections on our networks in 2013–2014 of 204% in manufacturing sector, 128% in finance and insurance, 120% for media and entertainment, and so forth.

Industrial reports state that, nowadays, we are living the highest increase in the number of connected devices and, most of all, they are not only PCs, laptops, TVs, smartphones,

C. Mariotti is with Infineon Technologies Austria AG, 9500 Villach, Austria (e-mail: chiara.mariotti@infineon.com).

F. Alimenti and L. Roselli are with the Department of Engineering, University of Perugia, 06123 Perugia, Italy.

M. M. Tentzeris is with the School of Electrical and Computer Engineering, Georgia Institute of Technology, Atlanta, GA 30332 USA.

or tablets, but also watches, glasses, wearables, medical equipment, and almost anything else very soon. The IoT is having impact on *everything*, and at some point, we expect *everything* to be connected in the Internet: the era of Internet of Everything (IoE) is beginning with a huge market by 2020 [3].

The idea behind IoT is that objects autonomously sense, collect, and wirelessly send the information to the network [4]–[7]. Having a huge amount of connected devices means also considering new challenges related to high-level protocols and communication [8], energy (no batteries and no cables), and integrability with the environment. Ideally, the most suitable device for IoT applications should be wireless, energy autonomous, and made of environmentally friendly and mechanically flexible materials [9]. In this way, the electronics can be integrated to the hosting object with a limited impact on the environment, on the fabrication process and cost, and on the end user, while they can be printed in large areas enabling a great scalability to large numbers [10]. These requirements can be pursued by introducing novel technologies and materials such as zero- or low-power architectures, wireless power transfer and energy harvesting [11], chipless solutions [7], [12], low-cost polymer-based substrates, and roll-to-roll (R2R) compatible industrial prototyping.

The focus of this paper is on the enabling technologies and, in particular, it has the purpose of demonstrating that RF passive elements can be fabricated by means of additive manufacturing (AM) processes reducing the costs and time of production with respect to traditional technologies, using unconventional, mechanically flexible, and environmentally friendly substrates (like photo-paper), and keeping high the RF performance of the component. In particular, in this paper, technologies like vertically integrated inkjet printing [13], [14] and metal adhesive laminate method [15], [16] are adopted. The choice of such technologies is suitable not only for the beforehand discussed motivations, but also for the perspective of their combination in an industrial (R2R) environment for high volume production of hardware in the IoT and large-area electronics application scenarios [10].

It is well known that inductors and capacitors are key components for the realization of many RF circuits (e.g., filters, matching networks, oscillators, resonators, and mixers) that are fundamental for wireless IoT nodes. The proposed technologies aim to effectively integrate these elements so that bulky

lumped components can be avoided. In this way, the costs and weight of the hosting systems are dramatically reduced, while better mechanical flexibility and eco-compatibility can be achieved: these aspects are of paramount importance when pursuing compatibility with objects' manufacturing [1]. In particular, with respect to [17], we show inductors and transformers with higher Q-factors fabricated on paper with the proposed processes.

This paper is divided into an illustration of the fundamental features of the proposed technologies (Section II), design and characterization of proof-of-concept RF passive components prototypes on paper substrates (Section III), and eventually the demonstration of their design (Sections IV–VI) and integration in a prototype of 1-GHz balanced mixer, realized on paper as well (Section VII).

## II. TECHNOLOGIES AND THEORY OF OPERATION

The growth of IoT market perspective and new applications is increasing the research to propose enabling technologies for high industrialization of the wireless nodes involved in such scenarios. The requirements for new technologies are independence on the hosting materials, mechanical flexibility, low cost, eco-compatibility, and fast prototyping. In the last decade, various candidate technologies have been identified to accomplish the prerequisites previously illustrated. Among others, there are gravure printing, screen printing, laser etching, inkjet printing [13], and metal adhesive laminate [10]. The last two will be described in the next sections since they have been adopted in this paper to demonstrate RF metal–insulator–metal (MIM) passives on cellulose-based substrate.

### A. Vertically Integrated Inkjet Printing

Planar circuits on cellulose-based substrates fabricated by means of nanoparticle silver inkjet printing have been already widely investigated and demonstrated [11], [13], [18] in the past. Recently, new dielectric inks have been developed and characterized in order to enable the realization of MIM structures: inductors on flexible LCP or paper [14], [17], capacitors on Kapton [19] or silicon [20], transformers on LCP [21], *LC* tank [22], and microelectromechanical systems [23].

Fig. 1 illustrates the basic steps of vertically integrated inkjet printing. In step 1, the first metal layer is deposited with a typical thickness of 0.5 $\mu$m per pass and with a curing temperature of 120 °C (this value can go up to 180 °C based on the thermal tolerance of the substrate). After creating the conductive film, a dielectric ink is selected based on the application (typically polymers like PVPh or SU-8 are adopted to realize the ink solution) and printed to obtain an insulating layer. The way of processing the dielectric films and their physical and RF properties are highly dependent on the type of polymer used [24]. The third step consists of the next metal layer printing and its baking to finalize the MIM component or prepare it for the next layer deposition.

The proof-of-concept components proposed in this paper are fabricated with the Dimatix DMP2800 platform that is typically used for rapid prototyping at laboratory level. The silver ink is provided by Advanced Nano Products (ANP).
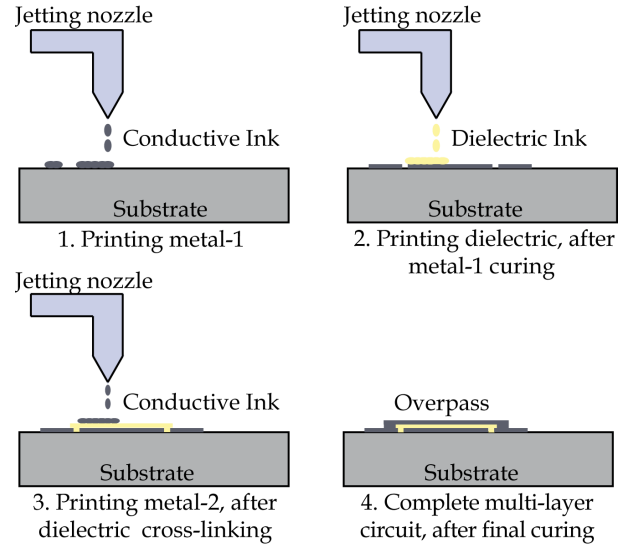


Fig. 1. Schematic of the fundamental features of vertically integrated inkjet printing.

The dielectric ink is composed of SU-8 2002 and 2005 (from Microchem) with a solid content by weight of 29% and 45%, respectively, dissolved in cyclopentanone in a 80%–20% ratio by weight in order to obtain a stable ink with a viscosity of 9 cP measured on a Gilmont falling ball viscometer [19]. The SU-8 ink is cross linked by exposition to UV rays and heating to 50 °C for 30 min. The typical realized thickness, with a drop spacing of 20 $\mu$m, is of about 4–5 $\mu$m per pass. The electrical permittivity is between 3 and 3.2, while the loss tangent is close to 0.04 for frequencies up to 25 GHz. The profile thickness is determined using a Dektak profilometer on square pads printed on top of rigid glass substrates.

The entire process is performed with 10-pL cartridges and a drop spacing of 20 $\mu$m. A more detailed description of the ink formulation and characterization is reported in [25].

### B. Copper Adhesive Laminate Method

The copper laminate method is described and characterized on paper substrates for frequencies up to 30 GHz in [15] and [16]. This technology adopts the lithography approach on adhesive copper tape and exploits its glue to attach the circuit on top of the substrates. Many circuits fabricated in this way are demonstrated in [26]–[32].

As it can be seen in Fig. 2, the key step of the process is to use a sacrificial layer, after the standard lithography procedure. This layer allows the protection film from the copper tape to be removed and to be attached it to the substrate by keeping constant the relative distances of the layout traces. This process is taking place at room temperature and is low cost, R2R compatible, substrate independent, and with a high metal conductivity (i.e., $5.8 \times 10^7$ S/m).

The substrate chosen for this paper is standard Mitsubishi photo-paper with a thickness of 230 $\mu$m, a dielectric constant ($\varepsilon_r$) equal to 2.9, and a loss tangent (tan $\delta$) of 0.06 at 1 GHz.

### C. RF Passive Components' Design and Analysis

All RF passive components' geometries have been first designed, simulated, and optimized using a full-wave
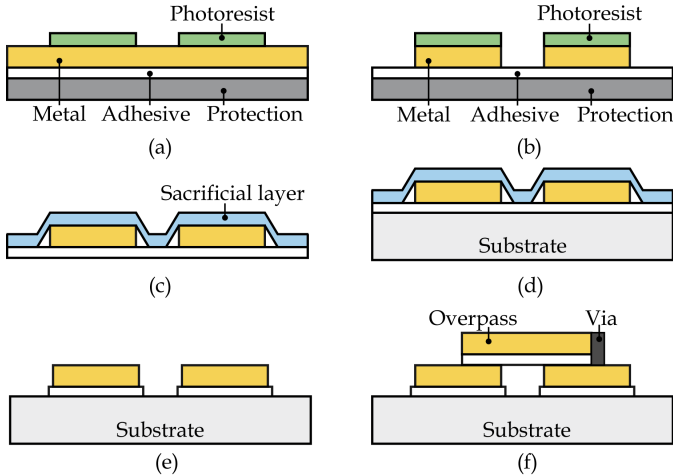
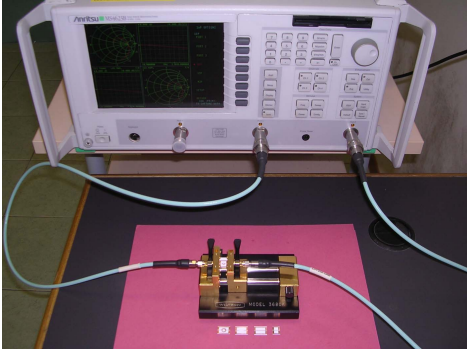Fig. 2. Illustration of the basic steps of the copper laminate method.



Fig. 3. Photograph of the experimental setup.

electromagnetic tool, in particular Computer Simulation Technology (CST) Microwave Studio (MS); then the prototypes have been fabricated and tested with a vector network analyzer, measuring the two-port S-parameters. The S-matrix is then elaborated with the equations reported in the following, relative to port 1 when port 2 is shorted to the ground:

$$L = \frac{\text{Im}\{1/Y_{11}\}}{2\pi f} \tag{1}$$

$$C = \frac{-1}{\text{Im}\{1/Y_{11}\}2\pi f} \tag{2}$$

$$R = \text{Re}\{1/Y_{11}\} \tag{3}$$

$$Q = \frac{|\text{Im}\{1/Y_{11}\}|}{R}. \tag{4}$$

In these equations, the S-matrix is converted into the Y-matrix, being $Y_{11} = Y(1, 1)$, and $R$ is the equivalent series resistance. The data postprocessing has been performed using Advanced Design Studio (ADS) to compare the measurements with the simulations, as it will be shown in the following. A picture of the experimental setup is reported in Fig. 3.

## III. INKJET-PRINTED RF PASSIVE COMPONENTS

This section describes the experimental results obtained for inkjet-printed RF, multilayer inductors, and capacitors on flexible paper substrates in configurations enabling their easy two-port integration in RF modules.
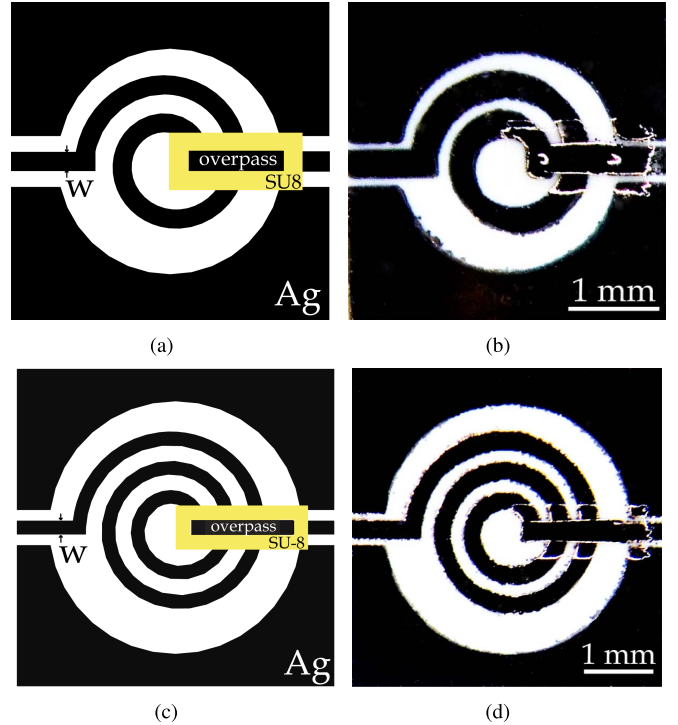


Fig. 4. Inkjet-printed MIM inductors. (a) and (c) Top view and (b) and (d) photograph of the prototypes for 1.5- and 2.5-turn design, respectively.
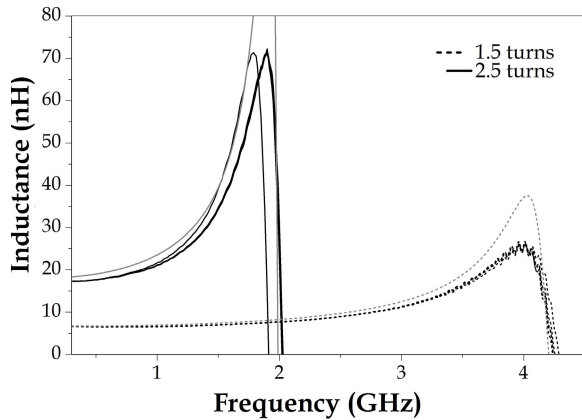
### A. MIM Inductors

In Fig. 4, the top view of the inductors' geometry [Fig. 4(a) and (c)] and the photographs of the prototypes [Fig. 4(b) and (d)] are reported for 1.5- and 2.5-turn designs, respectively. In both cases, the linewidth ($w$ in Fig. 4) and the spacing are set to 0.3 mm. Metalizations are made of five passes of nanoparticle silver ink from ANP, resulting in a 2.5-$\mu$m film; the dielectric to separate the metal levels is made of a four-pass printed SU-8 ink [19] with an overall thickness of 20 $\mu$m. The vias to connect metal 0 and metal 1 have been created by patterning holes in the SU-8 film in a way that the silver ink of the top metal could fill them and realize low-resistance contacts.

Fig. 5 shows the inductance ($L$) and the quality factor ($Q$) measured on five samples per design. The process is demonstrated to be highly repeatable, and a good agreement between measurement and simulated models is shown.

Inductance values of about 7 nH, maximum $Q$ of 11, and self-resonant frequency (SRF) of 4.25 GHz are exhibited by the 1.5-turn inductors. The 2.5-turn geometry is instead performing $L$ of 18 nH, maximum $Q$ of 10, and SRF around 2 GHz. It is confirmed, as expected from the inductors' theory, that larger geometries result in higher $L$ values and lower SRFs.

### B. MIM Capacitors

Inkjet-printed MIM capacitors' prototypes on photographic paper are discussed in this section. The geometry proposed, depicted in Fig. 6(a), consists of circular parallel-plate capacitors with a radius ($r$) of 0.5 mm and a CPW feeding structure.

(a)
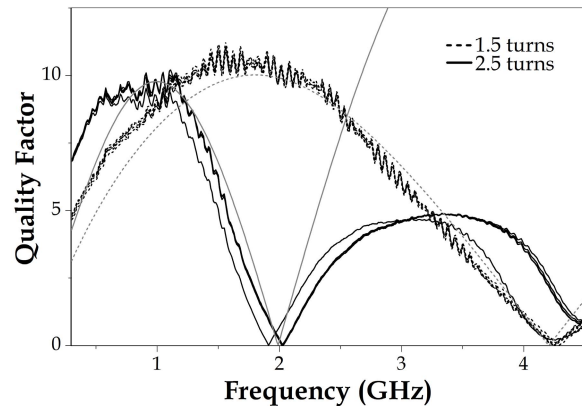


(b)

Fig. 5. RF performance of the printed inductors: dashed curves are for 1.5 turns, while solid lines are for 2.5 turns. Measurements of the five prototypes are in black, whereas simulations are shown in gray.
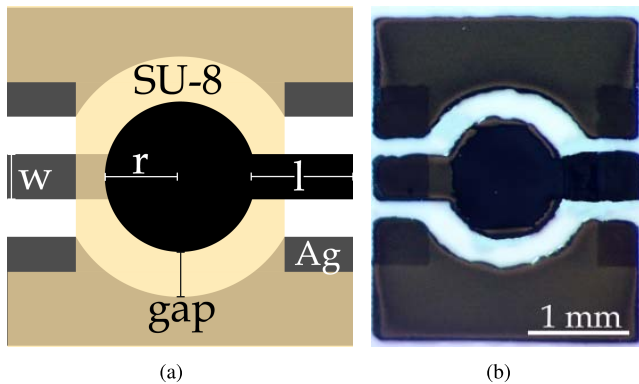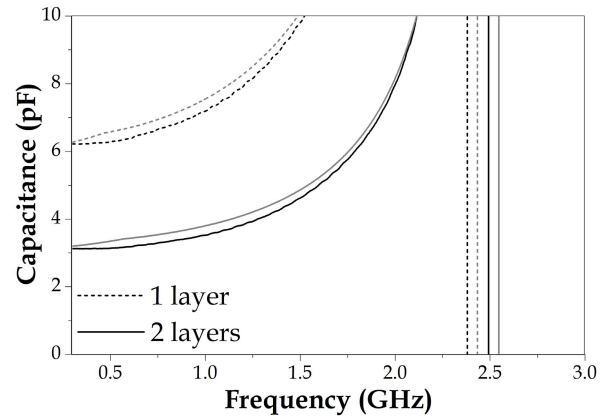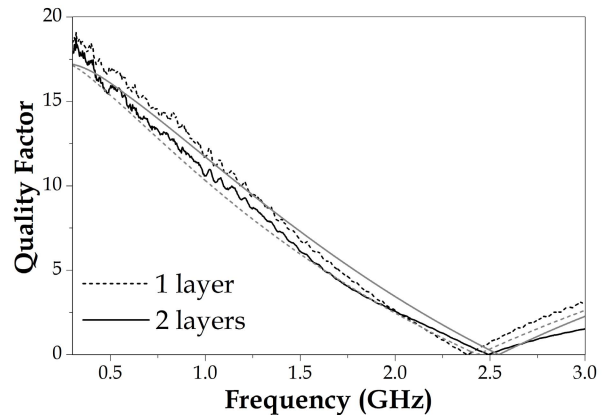


(a)



(b)

Fig. 7. RF performance of the inkjet-printed MIM capacitors, with one layer (dashed line) and two layers (solid line) of SU-8, in terms of (a) capacitance and (b) quality factor. Gray curves refer to simulations, while black curves are experimental.

in Fig. 7, where the simulated and experimental results are summarized for both samples with one and two layers of SU-8. Performance has been evaluated up to 3 GHz demonstrating a quality factor over 15 and the SRF of 2.5 GHz; moreover, a good agreement between the CAD model and the fabricated prototypes is shown.

## IV. COPPER ADHESIVE LAMINATE RF COMPONENTS ON PAPER

This section reports similar geometries of MIM passive components fabricated with the copper adhesive laminate technique on the same flexible cellulose-based substrate for comparison purposes. In this case, the insulator between two metal layers is just the acrylic adhesive layer provided with the copper laminate (original idea). Such an insulator has a thickness of 30 $\mu$m with a $\varepsilon_r = 2.45$.

### A. MIM Inductors

Spiral circular inductors are illustrated in this section: the geometries are shown in Fig. 8(a) and (b), while the micrographs of the fabricated samples are given in Fig. 8(c) and (d), for 1.5-turn and 2.5-turn structures, respectively. The metallic traces are 0.4 mm wide ($w$), while the gap between them is



(a)      (b)

Fig. 6. Inkjet-printed MIM capacitors. (a) Top view. (b) Photograph of the prototype. In the design, $r = 0.5$ mm, $w = 0.3$ mm, gap $= 0.25$ mm, and $l = 0.65$ mm.

The SU-8-based ink is printed as a dielectric film between the metal plates, with thicknesses of 4 (one pass) and 8 $\mu$m (two passes). The photo of an inkjet-printed prototype is shown in Fig. 6(b).

Considering the geometry and the properties reported for the adopted materials, the expected value of the capacitance for the fabricated prototypes has to be in the range of 2.5–6.5 pF. This fits very well with the values of the curves reported
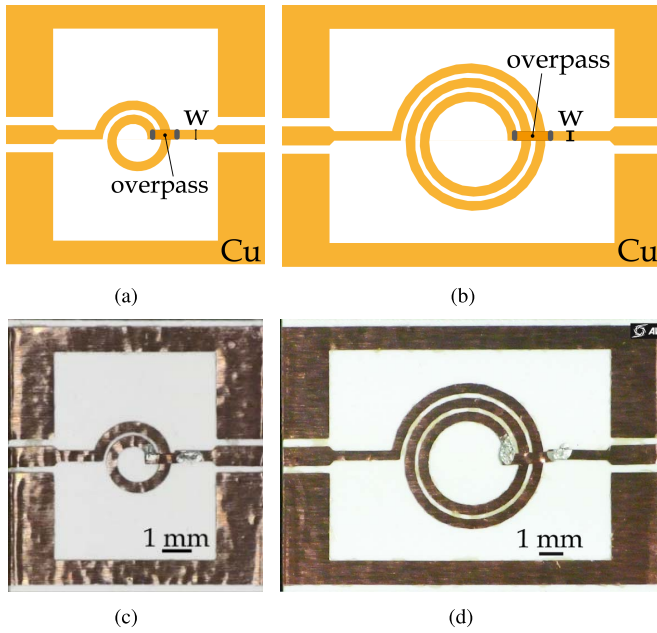
Fig. 8. Copper adhesive laminate MIM inductors. (a) and (b) Top view of the design and (c) and (d) micrographs of the prototypes, for the 1.5-turn and 2.5-turn design, respectively.
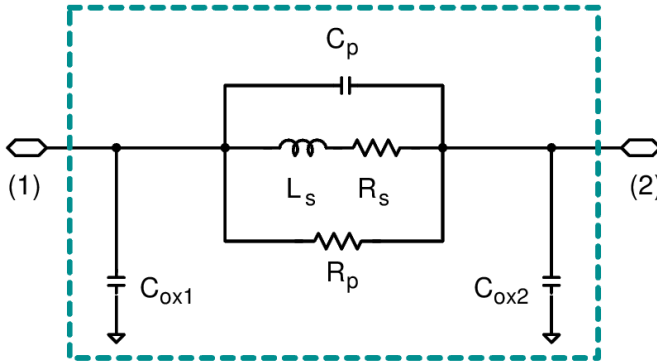


Fig. 9. Equivalent circuit of the inductors. In both geometries, $R_s = 0.6$ Ω, $C_p = 0.28$ pF, and $C_{ox1} = 0.05$, pF while $C_{ox2}$, $R_{sub}$, and $C_{sub}$ are 0. $R_p$ is 4 kΩ for the 1.5-turn inductor and 18 kΩ for the 2.5-turn one. $L_s$ is determined by (5).

equal to 0.2 mm. The outer diameters are 3.3 mm for 1.5 turns and 6.5 mm for 2.5 turns.

The S-parameters have been measured up to 4 GHz, and the devices exhibit inductance values of 7.5 and 41 nH and quality factors over 75 and 50, for 1.5-turn and 2.5-turn inductors, respectively.

An equivalent circuit model has also been developed based on the schematic in Fig. 9. As shown in the results in Fig. 10, such a fits the experimental results in a very accurate way (error below 8%).

The inductance value in Fig. 9, $L_s$, is obtained with the equation for planar spiral inductors reported in [33] is also performed. The formula is

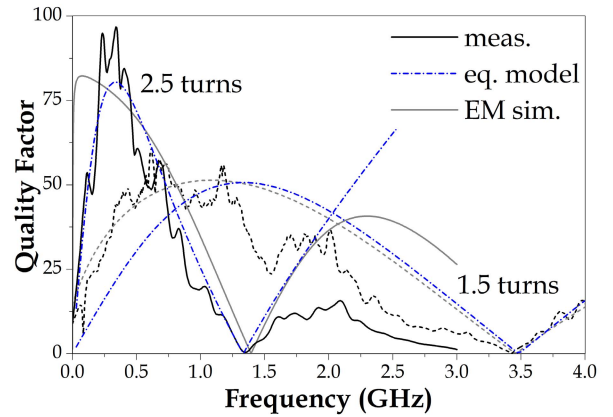$$L_s = \frac{\mu n^2 d_{\text{avg}} c_1}{2} (\ln(c_2/\rho) + c_3\rho + c_4\rho^2) \qquad (5)$$

where $n$ is the number of turns, $\mu$ is the permeability, the coefficients $c_i$ for circular designs are equal to 1.00, 2.46,

### TABLE I
EQUATION-BASED MODEL FOR COPPER INDUCTORS
BASED ON THE FORMULA IN [33]

| n | $d_{in}$ (mm) | $d_{out}$ (mm) | $w$ (mm) | $s$ (mm) | $L_{eq}$ (nH) |
|---|---|---|---|---|---|
| 1.5 | 1.3 | 3.3 | 0.4 | 0.2 | 7.5 |
| 2.5 | 3.3 | 6.5 | 0.4 | 0.2 | 41 |
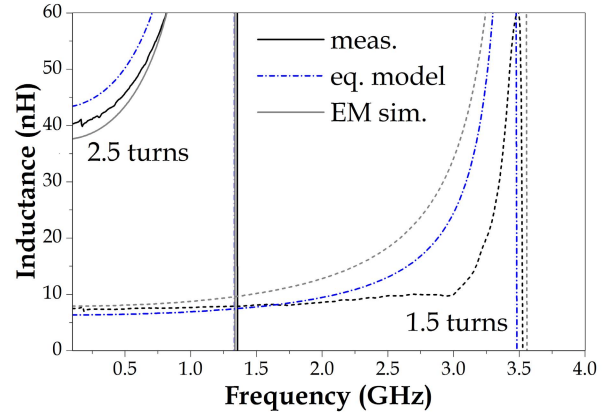


(a)



(b)

Fig. 10. RF performance of the copper inductors: dashed lines are for 1.5-turn designs, while solid lines are for the 2.5-turn geometries. EM simulations are in gray lines, while the equivalent model results are in blue dashed–dotted lines.

0.00, and 0.20, respectively, $d_{\text{avg}}$ is the average diameter defined as $0.5(d_{\text{out}} + d_{\text{in}})$, and $\rho$ is the fill ratio expressed by $(d_{\text{out}} - d_{\text{in}})/(d_{\text{out}} + d_{\text{in}})$.

The computed inductance values are reported in Table I.

Finally, it is worth underlining that the inductance values obtained with the copper adhesive laminate devices complement those of the inkjet-printed ones.

### B. MIM Capacitors

An MIM capacitor fabricated with copper laminate on paper is shown in Fig. 11(b), while its design is illustrated in Fig. 11(a). The top and bottom plates have edges = 2 mm (l1) and = 1.7 mm (l2), respectively. It is worth noting that the top plate is smaller than the one in the bottom to facilitate
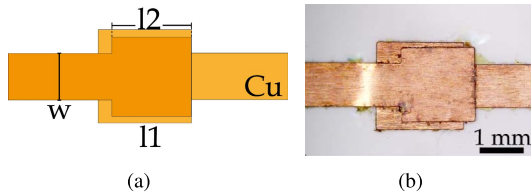
Fig. 11. Copper laminate MIM capacitor. (a) Top view. (b) Fabricated sample.
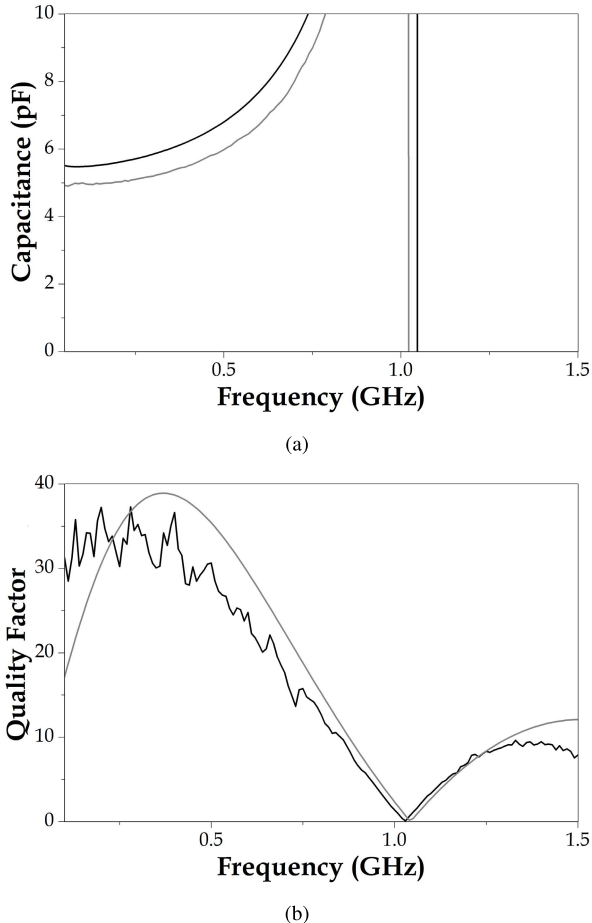


(a)



(b)

Fig. 12. Copper laminate MIM capacitor: RF performance. The max Q is over 30, and the SRF is 1 GHz. Simulations are in gray lines, while measurements are in black lines.

the alignment step and minimize the probability of accidental short circuits of the capacitor.

The sample is tested in the frequency range of 0.05–1.5 GHz. The SRF is close to 1 GHz, whereas the maximum Q is over 30 and the capacity value is 2.5 pF. The specific capacitance is about 1.25 pF/mm$^2$. The agreement between simulations and measurements is reasonable (see Fig. 12).

## V. SUMMARY OF RESULTS AND COMPARISON WITH THE STATE OF THE ART

In this section, a comparison with the state of the art of flexible inductors and capacitors, i.e., the standalone passive devices, is reported in Tables II and III, respectively.

As it can be seen from the data shown in Tables II and III, the performance of the inductors realized with the proposed

TABLE II
RF INDUCTORS ON PAPER: COMPARISON WITH THE STATE OF THE ART

| Ref | geometry | process | L (nH/mm$^2$) | maxQ |
|---|---|---|---|---|
| [34] | square | inkjet | 0.015 | n.a. |
| [35] | spiral | inkjet | 0.002 | n.a. |
| [36] | meander | inkjet | 0.27 | 25 |
| [37] | GaAs | octagonal | 96 | 20 |
| this work-1 | spiral | inkjet | 1.47 | 11 |
| this work-2 | spiral | copper lam. | 1 | 75 |

TABLE III
RF CAPACITORS ON PAPER: COMPARISON WITH THE STATE OF THE ART

| Ref | geometry | process | C (pF/mm$^2$) | maxQ |
|---|---|---|---|---|
| [35]-1 | square | inkjet | 0.74 | n.a. |
| [35]-2 | interdigit | inkjet | 0.016 | 0.004 |
| [37] | GaAs | square | 458 | 1000 |
| this work-1 | circular | inkjet | 6.5 | 15 |
| this work-2 | square | copper lam. | 1.25 | 35 |

technologies are two to three times higher than what is reported in the literature for similar geometries printed on flexible substrates [38]–[40]. Also for the capacitors, the Qs are two times higher compared with those already published [19].

Note that, in order to make the comparison with state of the art, the values per unit area have been computed with post-processing operations [de-embedding and math computation of L (or C)/A (nH (or pF)/mm$^2$)]

In general, despite the fact that the presented proof-of-concept designs are similar to what is shown in [14] and [19], they exhibit higher Qs on lossier substrate (i.e., standard photographic paper, $\tan\delta \approx 0.06$) than what is reported on more conventional materials as LCP and Kapton ($\tan\delta \approx 0.003$).

As a result, both proposed technologies are suitable for the fabrication of RF multilayer components and the difference in performance is, for instance, due to the different conductivity of the metals or the dielectric properties and thicknesses. However, an industrialization exploiting the benefits of both methods would be very beneficial for the integration of flexible components and circuits with IoT systems.

## VI. APPLICATION: RF MIXER ON PAPER SUBSTRATE

Several examples of high-performing passive components on flexible cellulose-based substrates have been presented in the previous sections; now, in order to demonstrate their usability for practical RF components and circuits, an RF mixer layout is proposed on paper substrate. The mixer operates in the UHF-RFID frequency band up to 1 GHz and uses a lumped balun transformer.

### A. Transformer Design and Characterization

First, the proof-of-concept transformer geometry has been developed and simulated through the full-wave tool MS, provided by CST for frequencies up to 5 GHz. The balun
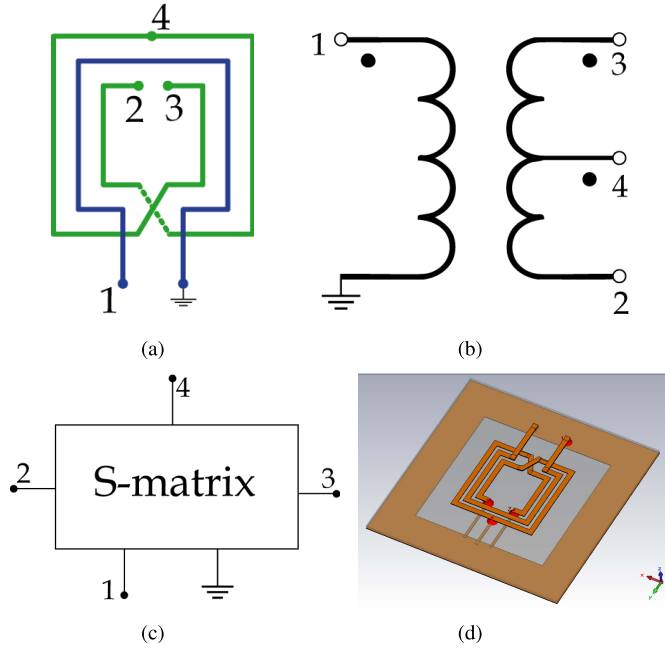
Fig. 13.   Transformer (a) schematic and (b) equivalent circuit. (c) Four-port model and (d) 3-D CST model, for simulation and characterization.

TABLE IV
BALUN SIMULATED PERFORMANCE AT 1 GHZ

|  | L (nH) | maxQ | SRF (GHz) |
|---|---|---|---|
| Primary (1) | 27 | 120 | 2.4 |
| Secondary (2) | 12.9 | 77 | 1.6 |
| Secondary (3) | 12.1 | 100 | 2.6 |
| Secondary (23) | 27.8 | 105 | 2.4 |



Fig. 14.   Balun transformer simulations in terms of (a) self-inductance and mutual inductances and (b) quality factors.

consists of a square single-turn primary and a square two-turn secondary.

For the transformer characterization, the primary is split into two halves on the right (see Fig. 13) where the mixer diodes will be placed (i.e., ports 2 and 3). The characterization of the transformer is performed by exporting the S-parameter file in ADS and simulating the schematic of Fig. 13. The self-inductance and mutual inductance and quality factors are determined adopting the series model as follows.

1) $L_1 = (\mathrm{Im}\{1/Y_{11}\}/2\pi f)$ and $Q_1 = (|\mathrm{Im}\{1/Y_{11}\}|/R_1)$, when port 1 is terminated in a 50-$\Omega$ load and all the other ports are left open.

2) $L_{2(3)} = (\mathrm{Im}\{1/Y_{22(33)}\}/2\pi f)$ and $Q_{2(3)} = (|\mathrm{Im}\{1/Y_{22(33)}\}|/R_{2(3)})$, when port 2 (3) is terminated in a 50-$\Omega$ load, port 4 is grounded, and port 1 is open.

3) $L_{23} = (\mathrm{Im}\{1/Y_{22(33)}\}/2\pi f)$ and $Q_{23} = (|\mathrm{Im}\{1/Y_{22(33)}\}|/R_{2(3)})$, when ports 2 and 3 are terminated in the same 50-$\Omega$ load and all the other ports are left open.

The results of the characterization are shown in Fig. 14 and summarized in Table IV at the frequency of interest for the mixer (i.e., 1. GHz).
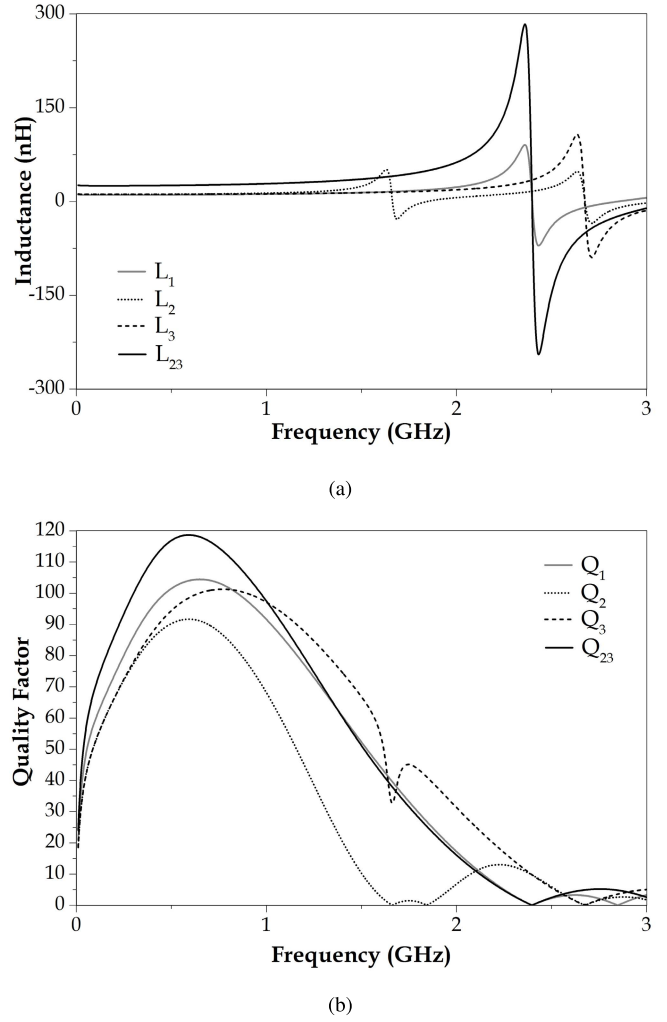
### B. Mixer Design and Test

The presented proof-of-concept singly balanced mixer subsystem prototype consists of a balun, the primary of which is connected to the LO, while the secondary center receives the RF. The other two secondary terminals (ports 2 and 3) are wired to two diodes (i.e., HSMS2850 from Avago Technologies), providing the required nonlinearity. Schematic and an illustration of the described circuit are shown in Fig. 15. Since the theory behind mixers' working principle is not the main aim of this paper and it is well known in the literature, the authors refer to [41] and [42] for a more detailed discussion of this type of circuit.

The mixer prototype has been optimized to work with an LO signal at 1 GHz and an RF signal at 900 MHz with a resulting IF of 100 MHz.

Once the transformer has been designed and characterized with full-wave simulations (see the previous paragraph), the S-parameters are imported in ADS in order to perform the harmonic balance simulation of the complete circuit in Fig. 15(a) and determine the conversion loss (CL) between the power available at RF and that delivered to the road. The circuit
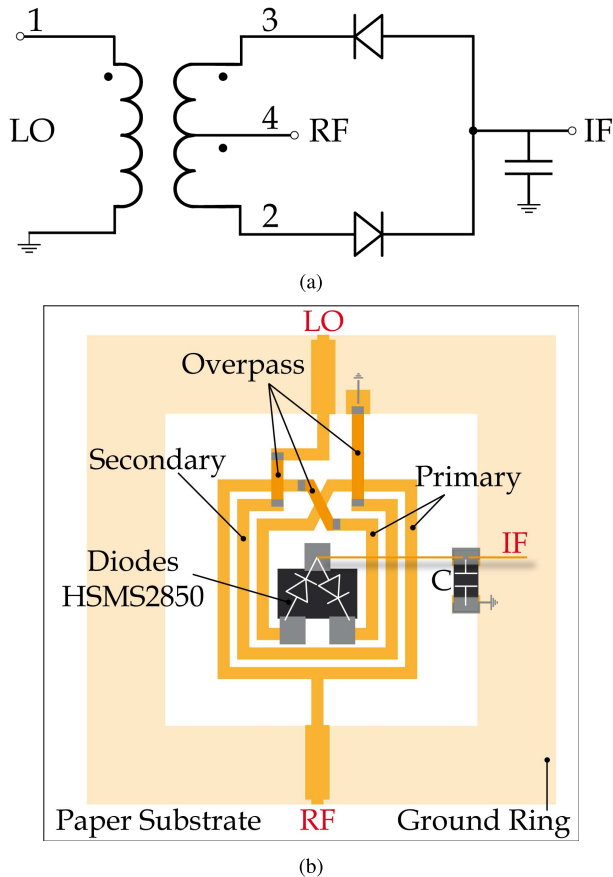
(a)



(b)

Fig. 15. Mixer (a) schematic and (b) illustration: a spiral transformer is connected to a series of diodes in a single-balanced mixer configuration. The output capacitance ($C$) is 4.7 pF.
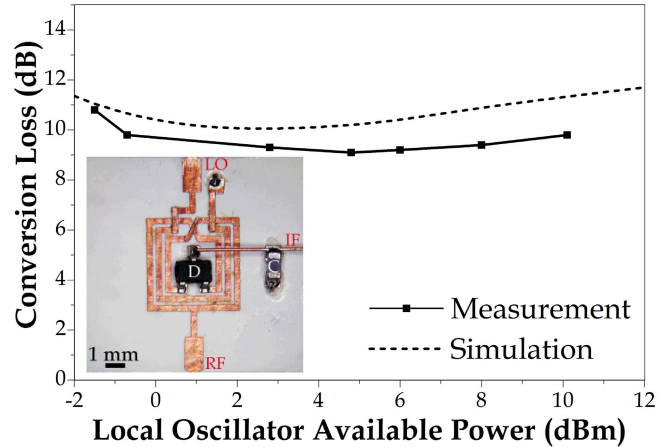


Fig. 16. Mixer test: measured and simulated CL (dB) versus LO available power (dBm). The photo of the prototype is also shown.

To the best of the authors' knowledge, this is the first mixer on cellulose substrates based on a lumped balun transformer. The total substrate area is only 25 mm$^2$, whereas the measured CLs compare well with those of other mixer circuit implemented with more performing technologies.

## VII. CONCLUSION

To summarize, this paper demonstrated, with models, simulations, and experiments, the use of novel technologies for on-paper mechanically flexible microwave passive components. Such processes exploit several additive steps with advantages in terms of low chemical waste, short time of production, and low costs. The RF performance is evaluated up to 6 GHz, and Qs over 70 are registered. The featured capacitance and inductance per unit area demonstrate an improvement of more than one order of magnitude compared with the state of the art of similar technologies on less lossy flexible substrates. In addition, in order to step up to a system-block level, a transformer is adopted to design and implement a $5 \times 5$ mm$^2$ single balanced mixer that exhibits a CL of less than 10 dB. In conclusion, the combination of the copper adhesive laminate process with inkjet printing would be an excellent manufacturing technology for the realization of flexible RF components and circuits in low-cost ordinary materials, such as cellulose-based paper, for a variety of IoT and "networked society" applications.

TABLE V

MIXER COMPARISON WITH THE STATE OF THE ART

| Ref | f (GHz) | minCL (dB) | Size | Technology |
|---|---|---|---|---|
| [43] | 2-7 | 9 | n.a. | GaAs |
| [44] | 6-6.5 | 8-10 | n.a. | CNC |
| [45] | 2-3 | 12 | 5 mm$^2$ | SiC MESFET |
| this work | 1 | 10 | 25 mm$^2$ | Cu on Paper |

simulation is performed considering the SPICE model of the diodes reported in the datasheet.

The device has been fabricated on paper substrate with the copper adhesive laminate method and tested with the HP8657A spectrum analyzer. Simulations and experiments are shown in Fig. 16, where the CL is reported in decibels. A difference of 1.1 dB in correspondence with the minimum CL is shown demonstrating an agreement between the measurement and the simulations of about 28%.

Moreover, it is worth noting that the tested IF-LO isolation is 50 dB.

A comparison with similar mixer topologies in traditional substrates and technologies is reported in Table V.

## REFERENCES

[1] D. Evans, "The Internet of Things how the next evolution of the Internet is changing everything," CISCO, San Jose, CA, USA, White Papers, 2011, p. 2.

[2] "The Internet of Things 2015," Verizon, New York, NY, USA, Tech. Rep., 2015.

[3] J. Bradley, C. Reberger, A. Dixit, and V. Gupta, "Internet of everything: A $4.6 trillion public-sector opportunity," CISCO, San Jose, CA, USA, White Papers, 2013, pp. 1–4.

[4] L. Atzori, A. Iera, and G. Morabito, "The Internet of Things: A survey," *Comput. Netw.*, vol. 54, no. 15, pp. 2787–2805, Oct. 2010.

[5] J. Manyika, M. Chui, J. Bughin, R. Dobbs, P. Bisson, and A. Marrs, "How the Internet of Things is more like the industrial revolution than the digital revolution," McKinsey Global Inst., Paris, France, Tech. Rep., 2013.

[6] I. G. Smith, "The Internet of Things 2012 new horizons," in *IERC European Research Cluster on the Internet of Things*, Halifax, U.K., 2012.

[7] S. Tedjini, N. Karmakar, E. Perret, A. Vena, R. Koswatta, and R. E-Azim, "Hold the chips: Chipless technology, an alternative technique for RFID," *IEEE Microw. Mag.*, vol. 14, no. 5, pp. 56–65, Jul. 2013.

[8] S. Lohr, *The Age of Big Data*. New York, NY, USA: The New York Times, Feb. 2012, p. 1.

[9] W. S. Wong, *Flexible Electronics*. Berlin, Germany: Springer, 2009.

[10] L. Roselli *et al.*, "Smart surfaces: Large area electronics systems for Internet of Things enabled by energy harvesting," *Proc. IEEE*, vol. 102, no. 11, pp. 1723–1746, Nov. 2014.

[11] S. Kim *et al.*, "No battery required: Perpetual RFID-enabled wireless sensors for cognitive intelligence applications," *IEEE Microw. Mag.*, vol. 14, no. 5, pp. 66–77, Jul. 2013.

[12] R. Nair, E. Perret, and S. Tedjini, "Temporal multi-frequency encoding technique for chipless RFID applications," in *IEEE MTT-S Int. Microw. Symp. Dig.,*, Montreal, QC, Canada, Jun. 2012, pp. 1–3.

[13] A. Rida, L. Yang, and M. M. Tentzeris, "Design and characterization of novel paper-based inkjet-printed UHF antennas for RFID and sensing applications," in *Proc. IEEE Int. Antennas Propag. Symp.*, Honolulu, HI, USA, Jun. 2007, pp. 2749–2752.

[14] B. S. Cook *et al.*, "Inkjet-printed, vertically-integrated, high-performance inductors and transformers on flexible LCP substrate," in *IEEE MTT-S Int. Microw. Symp. Dig.*, Jun. 2014, pp. 1–4.

[15] F. Alimenti, P. Mezzanotte, M. Dionigi, M. Virili, and L. Roselli, "Microwave circuits in paper substrates exploiting conductive adhesive tapes," *IEEE Microw. Wireless Compon. Lett.*, vol. 22, no. 12, pp. 660–662, Dec. 2012.

[16] C. Mariotti *et al.*, "Modeling and characterization of copper tape microstrips on paper substrate and application to 24 GHz branch-line couplers," in *Proc. 43rd Eur. Microw. Conf.*, Nuremberg, Germany, Oct. 2013, pp. 794–797.

[17] C. Mariotti, B. S. Cook, F. Alimenti, L. Roselli, and M. M. Tentzeris, "Additively manufactured multilayer high performance RF passive components on cellulose substrates for Internet-of-Things electronic circuits," in *IEEE MTT-S Int. Microw. Symp. Dig.*, May 2015, pp. 1–4.

[18] V. Subramanian *et al.*, "Progress toward development of all-printed RFID tags: Materials, processes, and devices," *Proc. IEEE*, vol. 93, no. 7, pp. 1330–1338, Jul. 2005.

[19] B. S. Cook, J. R. Cooper, and M. M. Tentzeris, "Multi-layer RF capacitors on flexible substrates utilizing inkjet printed dielectric polymers," *IEEE Microw. Wireless Compon. Lett.*, vol. 23, no. 7, pp. 353–355, Jul. 2013.

[20] C. Mariotti, B. S. Cook, L. Roselli, and M. M. Tentzeris, "State-of-the-art inkjet-printed metal-insulator-metal (MIM) capacitors on silicon substrate," *IEEE Microw. Wireless Compon. Lett.*, vol. 25, no. 1, pp. 13–15, Jan. 2015.

[21] C. Mariotti, L. Aluigi, T. T. Thai, F. Alimenti, L. Roselli, and M. M. Tentzeris, "A fully inkjet-printed 3D transformer balun for conformal and rollable microwave applications," in *Proc. IEEE Antennas Propag. Soc. Int. Symp. (APSURSI)*, Jul. 2014, pp. 330–331.

[22] R. C. Roberts and N. C. Tien, "Multilayer passive RF microfabrication using jet-printed au nanoparticle ink and aerosol-deposited dielectric," in *Proc. 17th IEEE Int. Conf. Solid-State Sens., Actuators Microsyst. (TRANSDUCERS EUROSENSORS XXVII)*, Barcelona, Spain, Jun. 2013, pp. 178–181.

[23] S. B. Fuller, E. J. Wilhelm, and J. M. Jacobson, "Ink-jet printed nanoparticle microelectromechanical systems," *J. Microelectromech. Syst.*, vol. 11, no. 1, pp. 54–60, Feb. 2002.

[24] B. K. Tehrani, C. Mariotti, B. S. Cook, L. Roselli, and M. M. Tentzeris, "Development, characterization, and processing of thin and thick inkjet-printed dielectric films," *Organic Electron.*, vol. 29, pp. 135–141, Feb. 2016.

[25] J. G. Hester *et al.*, "Additively manufactured nanotechnology and origami-enabled flexible microwave electronics," *Proc. IEEE*, vol. 103, no. 4, pp. 583–606, Apr. 2015.

[26] M. Poggiani *et al.*, "24-GHz patch antenna array on cellulose-based materials for green wireless Internet applications," *IET Sci., Meas. Technol.*, vol. 8, no. 6, pp. 342–349, 2014.

[27] F. Alimenti, C. Mariotti, P. Mezzanotte, M. Dionigi, M. Virili, and L. Roselli, "A 1.2 V, 0.9 mW UHF VCO based on hairpin resonator in paper substrate and Cu adhesive tape," *IEEE Microw. Wireless Compon. Lett.*, vol. 23, no. 4, pp. 214–216, Apr. 2013.

[28] F. Alimenti *et al.*, "24 GHz single-balanced diode mixer exploiting cellulose-based materials," *IEEE Microw. Wireless Compon. Lett.*, vol. 23, no. 11, pp. 596–598, Nov. 2013.

[29] V. Palazzi *et al.*, "Low-power frequency doubler in cellulose-based materials for harmonic RFID applications," *IEEE Microw. Wireless Compon. Lett.*, vol. 24, no. 12, pp. 896–898, Dec. 2014.

[30] C. Mariotti, R. Gonçalves, L. Roselli, N. B. Carvalho, and P. Piño, "'Energy evaporation': The new concept of indoor systems for WPT and EH embedded into the floor," in *IEEE MTT-S Int. Microw. Symp. Dig.*, Phoenix, AZ, USA, May 2015, pp. 1–4.

[31] F. Alimenti *et al.*, "24-GHz CW radar front-ends on cellulose-based substrates: A new technology for low-cost applications," in *IEEE MTT-S Int. Microw. Symp. Dig.*, Phoenix, AZ, USA, May 2015, pp. 1–4.

[32] V. Palazzi *et al.*, "Demonstration of a high dynamic range chipless RFID sensor in paper substrate based on the harmonic radar concept," in *IEEE MTT-S Int. Microw. Symp. Dig.*, Phoenix, AZ, USA, May 2015, pp. 1–4.

[33] S. S. Mohan, M. del Mar Hershenson, S. P. Boyd, and T. H. Lee, "Simple accurate expressions for planar spiral inductances," *IEEE J. Solid-State Circuits*, vol. 34, no. 10, pp. 1419–1424, Oct. 1999.

[34] H. Lee, M. M. Tentzeris, Y. Kawahara, and A. Georgiadis, "Novel inkjet-printed ferromagnetic-based solutions for miniaturized wireless power transfer (WPT) inductors and antennas," in *Proc. Int. Symp. Antennas Propag. (ISAP)*, Nagoya, Japan, Oct. 2012, pp. 14–17.

[35] S. M. Bidoki, J. Nouri, and A. A. Heidari, "Inkjet deposited circuit components," *J. Micromech. Microeng.*, vol. 20, no. 5, p. 055023, 2010.

[36] H. Lee, B. S. Cook, K. P. Murali, M. Raj, and M. M. Tentzeris, "Inkjet printed high-Q RF inductors on paper substrate with ferromagnetic nanomaterial," *IEEE Microw. Wireless Compon. Lett.*, vol. 26, no. 6, pp. 419–421, Jun. 2016.

[37] Y. H. Jung *et al.*, "High-performance green flexible electronics based on biodegradable cellulose nanofibril paper," *Nature Commun.*, vol. 6, pp. 1–11, May 2015.

[38] G. McKerricher, J. Gonzalez, and A. Shamim, "All inkjet printed 3D microwave capacitors and inductors with vias," in *IEEE MTT-S Int. Microw. Symp. Dig.*, Seattle, WA, USA, Jun. 2013, pp. 1–3.

[39] A. Menicanin, L. Zivanov, M. Damnjanovic, A. Maric, and N. Samardzic, "Ink-jet printed CPW inductors in flexible technology," in *Proc. 35th Int. Conv. MIPRO*, Opatija, Croatia, May 2012, pp. 233–236.

[40] A. B. Menicanin, L. D. Zivanov, M. S. Damnjanovic, and A. M. Maric, "Low-cost CPW meander inductors utilizing ink-jet printing on flexible substrate for high-frequency applications," *IEEE Trans. Electron Devices*, vol. 60, no. 2, pp. 827–832, Feb. 2013.

[41] S. A. Maas, *Nonlinear Microwave and RF Circuits*, 2nd ed. Norwood, MA, USA: Artech House, 2003.

[42] S. A. Maas, *The RF and Microwave Circuit Design Cookbook*. Norwood, MA, USA: Artech House, 1998.

[43] B. Maity, P. K. Sethy, and K. Bandyopadhyay, "Design of a single balanced diode mixer with high LO/RF and LO/IF isolation in C-band test loop translator," in *Proc. IEEE Int. Conf. Adv. Commun. Control Comput. Technol. (ICACCCT)*, Aug. 2012, pp. 14–17.

[44] A. Maalik and Z. Mahmood, "A novel C-band single diode mixer with ultra high LO/RF and LO/IF isolation," in *Proc. Int. Conf. Elect. Eng.*, Coimbra, Portugal, Apr. 2007, pp. 1–6.

[45] M. Sudow, K. Andersson, P. A. Nilsson, and N. Rorsman, "A highly linear double balanced Schottky diode S-band mixer," *IEEE Microw. Wireless Compon. Lett.*, vol. 16, no. 6, pp. 336–338, Jun. 2006.

**Chiara Mariotti** (GS'12–M'13) was born in Perugia, Italy, in 1987. She received the Laurea degree (*magna cum laude*) in electronics and telecommunication engineering and the Ph.D. degree from the University of Perugia, Perugia, in 2011 and 2016, respectively, where she was involved in the development of substrate-independent fabrication processes and materials for RF and wireless Internet-of-Things applications.

In 2012, she joined the ATHENA Laboratory, Georgia Institute of Technology (GIT), Atlanta, GA, USA, where she was involved in flexible, inkjet printed electronics, and RFIDs for sensing/localization purposes. From 2013 to 2014, she spent another six months in Atlanta with a focus on mulitlayer inkjet printing solutions, such as process and inks, for RF passives and microfluidic devices. She was also a Visiting Researcher with the Institute of Telecommunications, Aveiro, Aveiro, Portugal, where she was involved in indoor wireless power transfer solutions. She is currently a Research and Development Engineer with Infineon Technologies Austria AG, Villach, Austria, where she is involved in the development of low-cost, hybrid, and highly integrated terahertz platforms, within a H2020 funded European Project, namely, M3TERA. She has co-authored 38 peer-reviewed papers and two book chapters with 216 citations in scholar.

Dr. Mariotti presented several conference papers and was a recipient of the Best Student Paper Award at the 2014 IEEE Wireless Power Transfer Conference. In 2011, she was recognized as the Student of the Year for the University of Perugia. She gave lectures at GIT. She was a Teaching Assistant in Perugia. She is a Reviewer for IEEE MICROWAVE WIRELESS AND COMPONENTS LETTERS, *Organic Electronics* (Elsevier), the Cambridge University Press, and international conferences.

**Federico Alimenti** (S'91–A'97–M'06–SM'09) received the Laurea and Ph.D. degrees in electronic engineering from the University of Perugia, Perugia, Italy, in 1993 and 1997, respectively.

From 2011 to 2014, he was the Scientific Coordinator of the ENIAC ARTEMOS Project. In 2014, he was a Visiting Professor with the École Polytechnique Fédérale de Lausanne, Lausanne, Switzerland. In 1996, he was a Visiting Scientist with the Technical University of Munich, Munich Germany. Since 2001, he has been with the Department of Engineering, University of Perugia, where he teaches the class "Microwave Electronics." He has co-authored two patents and over 200 papers in journals and conferences. He has an H-index of 18 in Google Scholar. His current research interests include microwave integrated circuit design and electronics on cellulose.

Dr. Alimenti was a recipient of the URSI Young Scientist Award in 1996 and the IET Premium (Best Paper) Award in 2013. He was the TPC Chair of the IEEE Wireless Power Transfer Conference in 2013.

**Luca Roselli** (M'92–SM'01) joined the University of Perugia, Perugia, Italy, in 1991. In 2000, he founded the spin-off WiS Srl. He was involved in electronic technologies for Internet of Things for six years. He is currently a Qualified Full Professor with the University of Perugia, where he teaches applied electronics and coordinates the HFE-Laboratory. He has authored over 280 contributions (H-i 23, i10 51, over 2000 citations-Scholar) and the books *Green RFID System* (Cambridge Univ. Press) and *Internet of Things Technologies* (Cambridge Univ. Press, 2017). His current research interests include HF electronic systems with a special attention to RFID, new materials, and wireless power transfer.

Prof. Roselli was a member of the Board of Directors of ART srl, Urbino, Italy, from 2008 to 2012. He is a member of the list of experts of the Italian Ministry of Research, the Past Chair of the IEEE Technical Committees MTT-24-RFID, the Vice-Chair of 25-RF Nanotechnologies, the 26-Wireless Power Transfer, the ERC Panel PE7, the Advisory Committee of the IEEE-WPTC, and the Chairman of the SC-32 of IMS. He is the Co-Chair of the IEEE Wireless Sensor Network Conference. He organized the VII Computational Electromagnetic Time Domain in 2007 and the first IEEE-Wireless Power Transfer Conference in 2013. He is an Associate Editor of *IEEE Microwave Magazine*. He is involved in the boards of several international conferences. He is a Reviewer for many international reviews, including the PROCEEDINGS OF THE IEEE, the IEEE TRANSACTIONS ON MICROWAVE THEORY AND TECHNIQUES, and IEEE MICROWAVE AND WIRELESS COMPONENTS LETTERS.

**Manos M. Tentzeris** (S'94–M'98–SM'03–F'10) received the Diploma degree (*magna cum laude*) in electrical and computer engineering from the National Technical University of Athens, Athens, Greece, and the M.S. and Ph.D. degrees in electrical engineering and computer science from the University of Michigan, Ann Arbor, MI, USA.

He is currently a Ken Byers Professor of Flexible Electronics with the School of Electrical and Computer Engineering, Georgia Institute of Technology College of Engineering, Atlanta, GA, USA. He was a Visiting Professor with the Technical University of Munich, Munich, Germany, in 2002, a Visiting Professor with GTRI-Ireland, Athlone, Ireland, in 2009, and a Visiting Professor with LAAS-CNRS, Toulouse, France, in 2010. He has given more than 100 invited talks to various universities and companies all over the world. He has helped to develop academic programs in 3-D/inkjet-printed RF electronics and modules, flexible electronics, origami and morphing electromagnetics, highly integrated/multilayer packaging for RF and wireless applications using ceramic and organic flexible materials, paper-based RFID's and sensors, wireless sensors and biosensors, wearable electronics, Green electronics, energy harvesting and wireless power transfer, nanotechnology applications in RF, microwave MEMs, and SOP-integrated (UWB, multiband, millimeter-wave, conformal) antennas. He served as the Head of the GT-ECE Electromagnetics Technical Interest Group, the Associate Director of the Georgia Electronic Design Center for RFID/Sensors research, the Associate Director of the Georgia Tech NSF-Packaging Research Center for RF Research, and the RF Alliance Leader. He heads the ATHENA Research Group (20 researchers), Riverside, CA, USA. He has authored over 620 papers in refereed journals and conference proceedings, five books, and 25 book chapters.

Dr. Tentzeris is a member of the URSI-Commission D, the MTT-15 Committee, and the Technical Chamber of Greece. He is an Associate Member of EuMA and a Fellow of the Electromagnetic Academy. He was a recipient or co-recipient of the 2015 IET Microwaves, Antennas and Propagation Premium Award, the 2014 Georgia Tech ECE Distinguished Faculty Achievement Award, the 2014 IEEE RFID-TA Best Student Paper Award, the 2013 IET Microwaves, Antennas and Propagation Premium Award, the 2012 FiDiPro Award in Finland, the iCMG Architecture Award of Excellence, the 2010 IEEE Antennas and Propagation Society Piergiorgio L. E. Uslenghi Letters Prize Paper Award, the 2011 International Workshop on Structural Health Monitoring Best Student Paper Award, the 2010 Georgia Tech Senior Faculty Outstanding Undergraduate Research Mentor Award, the 2009 IEEE Transactions on Components and Packaging Technologies Best Paper Award, the 2009 E. T. S. Walton Award from the Irish Science Foundation, the 2007 IEEE APS Symposium Best Student Paper Award, the 2007 IEEE IMS Third Best Student Paper Award, the 2007 ISAP 2007 Poster Presentation Award, the 2006 IEEE MTT Outstanding Young Engineer Award, the 2006 Asia–Pacific Microwave Conference Award, the 2004 IEEE TRANSACTIONS ON ADVANCED PACKAGING Commendable Paper Award, the 2003 NASA Godfrey Art Anzic Collaborative Distinguished Publication Award, the 2003 IBC International Educator of the Year Award, the 2003 IEEE CPMT Outstanding Young Engineer Award, the 2002 International Conference on Microwave and Millimeter-Wave Technology Best Paper Award, Beijing, China, the 2002 Georgia Tech-ECE Outstanding Junior Faculty Award, the 2001 ACES Conference Best Paper Award, the 2000 NSF CAREER Award, and the 1997 Best Paper Award of the International Hybrid Microelectronics and Packaging Society. He was the TPC Chair for the IEEE IMS 2008 Symposium and the Chair of the 2005 IEEE CEM-TD Workshop. He is the Vice-Chair of the RF Technical Committee (TC16) of the IEEE CPMT Society. He is the Founder and the Chair of the RFID Technical Committee (TC24) of the IEEE MTT-S, and the Secretary/Treasurer of the IEEE C-RFID. He is an Associate Editor of the IEEE TRANSACTIONS ON MICROWAVE THEORY AND TECHNIQUES, the IEEE TRANSACTIONS ON ADVANCED PACKAGING, and the *International Journal on Antennas and Propagation*. He was an IEEE MTT-S Distinguished Microwave Lecturer from 2010 to 2012. He is one of the IEEE CRFID Distinguished Lecturers.